Nonlinear Evolution of the Modulational Instability of Whistler Waves

V. I. Karpman,[a] F. R. Hansen, T. Huld, J. P. Lynov, H. L. Pécseli, and J. Juul Rasmussen
Association EURATOM–Risø National Laboratory, Physics Department, Risø National Laboratory, P.O. Box 49, DK-4000 Roskilde, Denmark
(Received 6 October 1989)

The nonlinear evolution of the modulational instability of whistler waves coupled to fast magnetosonic waves is investigated in two spatial dimensions by numerical simulations. The long-time evolution of the modulational instability shows a quasirecurrent behavior with a slow spreading of the energy, originally confined to the lowest wave numbers, to larger and larger wave numbers, resulting in an apparently chaotic or random wave field.

PACS numbers: 52.35.Mw, 52.35.Hr

Finite-amplitude whistler waves propagating along the magnetic field in a low-β plasma are modulationally unstable with respect to low-frequency perturbations.[1,2] Whistlers play an important role in the dynamics of magnetospheric plasmas. Both naturally occurring whistlers and whistlers used in active experiments may have amplitudes large enough for the modulational instability to be of significance (e.g., Ref. 3) and some observations may be interpreted in terms of modulational instabilities, although the evidence is not conclusive.[4] The nonlinear evolution of whistlers is generally described by a set of three coupled equations: a nonlinear Schrödinger-type equation for the whistler-wave amplitude and MHD equations including the effects of ponderomotive forces for the low-frequency response.[2] Considering the different branches of the modulational instability (MI) separately, Karpman and Stenflo[5] derived simplified equations for the evolution on each branch. We have employed the reduced model for a numerical investigation of the long-time nonlinear evolution of the two-dimensional MI of whistlers coupled to fast magnetosonic waves (FMS branch).

The purpose of the investigation was first to verify that the results from the reduced model agree with results based on the full model.[2] Then we verified the predicted recurrence, and the main subject of the present Letter is to study the long-time dynamics in detail, which indeed is feasible within the present simplified model. We found that the MI evolves in a quasirecurrent manner. For relatively low amplitudes we obtained a series of modulation and demodulation cycles with a slow spreading of the energy to higher modulation wave numbers. As the carrier-wave amplitude was increased, the recurrence periods became fewer and the energy spread faster to the higher mode numbers; i.e., the randomization became more effective.

Although our results are obtained for a model with specific applications to the evolution of whistlers, we believe that they are of fundamental interest for the nonlinear evolution of the modulation of waves in anisotropic, dispersive media. The one-dimensional MI of, e.g., deep water waves was clearly demonstrated to be recurrent.[6] The two-dimensional evolution of the MI of deep water waves, as described by a cubic Schrödinger equation, showed a quasirecurrent behavior with a successive leakage of energy to higher mode numbers.[7] This is somewhat similar to the results in this Letter for a more complex system.

Our numerical investigations are based on a two-dimensional version of the reduced equations for the FMS branch,[5,8]

$$i(\psi_t + v\psi_z) + \tfrac{1}{2}(s_1\psi_{xx} + s_2\psi_{zz}) = C_1 v\psi , \tag{1}$$

$$v_{tt} - C^2\nabla^2 v = C_2 |\psi|^2_{xx}, \quad b \approx v , \tag{2}$$

where $\psi = (E_x - iE_y)/E_0$ is the normalized, slowly varying whistler-wave electric field, $v = (n - n_0)/n_0$, with n the slowly varying density, and $b = (B_z - B_0)/B_0$, with B_z the slowly varying ambient magnetic field. The spatial coordinates are normalized with k_0, the wave number of the whistler wave, and time is normalized with the whistler-wave frequency ω. The coefficients in (1) and (2) are expressed in terms of $u = \omega/\omega_c$, where ω_c is the electron cyclotron frequency:

$$E_0 = \left[\frac{8m_i u(1-u)}{m_e}\right]^{1/2} \frac{c_A B_0}{c}, \quad c_A^2 = \frac{B_0^2}{4\pi n_0 m_i},$$

$$v = v_g/v_{ph} = 2(1-u), \quad s_1 = 1 - 2u,$$

$$s_2 = 2(1-u)(1-4u),$$

$$C = \frac{c_A}{v_{ph}} = \left[\frac{m_e/m_i}{u(1-u)}\right]^{1/2}, \quad C_1 = u,$$

$$C_2 = uC^2/(1-u).$$

Here v_{ph} and v_g are the whistler-wave phase velocity and group velocity, respectively, and c_A is the Alfvén velocity.

The dispersion relation for the MI of the whistler is found by linearizing Eqs. (1) and (2) around the stationary solution $\psi = \psi_0$, $v = 0$. We consider perturbations of the form $\psi = [\psi_0 + \phi(\xi)]\exp i\theta(\xi)$, where ψ_0, ϕ, and θ are real functions, $\xi = K_x x + K_z z - \Omega t$, and we take $\phi(\xi) = \mathrm{Re}[a\exp(i\xi)]$. The growth rate of the MI is maximum for wave numbers satisfying $KC - K_z v \approx -\frac{1}{2} \times (s_1 K_x^2 + s_2 K_z^2)$ and the corresponding value of $\Omega = \Omega_0 + i\gamma$ is approximately given as

$$\Omega_0 \approx KC, \quad \gamma \approx [(C_1 C_2)^{1/2}/(2KC)^{1/2}] K_x \psi_0 . \tag{3}$$

Equations (1) and (2) are solved numerically in a two-dimensional domain of size $L_x \times L_z$ with periodical boundary conditions. We employed a fully de-aliased spectral method.[9] The accuracy of the calculations was checked by monitoring the simple conserved quantities of Eqs. (1) and (2): $I_1 = \int_0^{L_x}\int_0^{L_z} |\psi|^2 dz\,dx$, $I_2 = \int_0^{L_x}\int_0^{L_z} \nu\,dz\,dx$. For all the results referred to, the relative variation of I_1 was less than 10^{-5}, and the absolute variation of I_2, which is zero for the applied initial conditions, was less than 10^{-18}.

As initial conditions we use a modulation which is a standing wave in the x direction and a propagating wave in the z direction, with wave numbers $K_{x0} = 2\pi/L_x$ and $K_{z0} = 2\pi/L_z$, and we choose the ratio K_{z0}/K_{x0} which gives the maximum growth rate γ at the given value of K_0. Further, the initial values for ϕ, θ, and ν are chosen to coincide with the linear evolution[2] of the MI:

$$\phi = 2a\exp(\gamma t)\cos(K_x x)\cos(K_z z - \Omega_0 t)\,,$$

$$\theta = \frac{4a\exp(\gamma t)}{\psi_0}\left[-\tfrac{1}{2}\sin(K_z z - \Omega_0 t) + \frac{\gamma}{s_1 K_x^2 + s_2 K_z^2}\cos(K_z z - \Omega_0 t)\right]\cos(K_x x)\,, \tag{4}$$

$$\nu = \frac{2a\psi_0 C_2 K_x^2 \exp(\gamma t)}{\gamma C K}\cos(K_x x)\sin(K_z z - \Omega_0 t)\,.$$

First, we show an example of a persistent recurrent behavior in Figs. 1 and 2. The parameters are similar to those used by Karpman and Shagalov.[2] An almost perfect recurrence is observed for the two recurrence periods shown. Continuing the calculations to larger times (up to $T = 50000$) we observed up to five recurrence periods, but the recurrence becomes more and more imperfect. From the development of the corresponding wave-number spectra we found that during the first recurrence periods the wave energy is confined to a few modes with the main part in the fundamental mode. As the recurrence gets less and less perfect the energy is spread among an increasing number of modes. The evolution in Figs. 1 and 2 coincides with the evolution found by Karpman and Shagalov[2] based on the complete set of

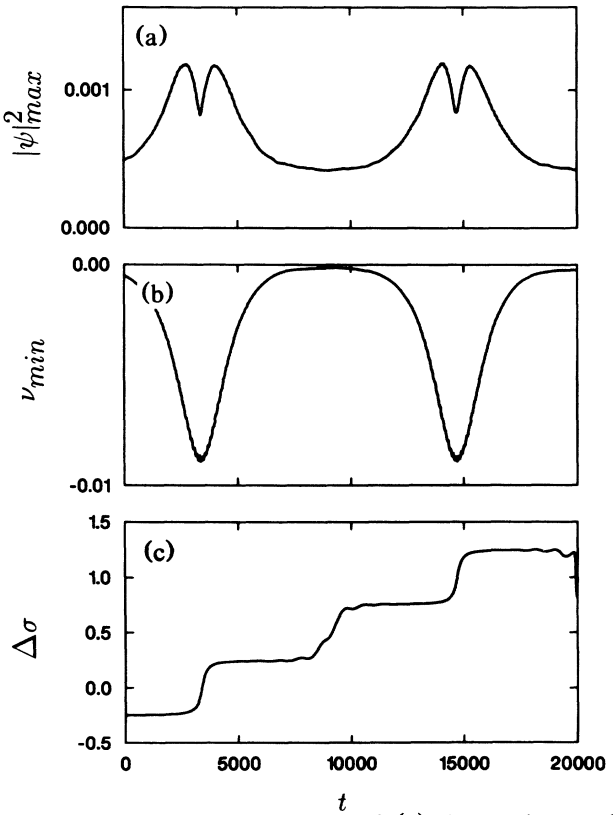

FIG. 1. The temporal evolution of (a) the maximum of $|\psi|^2$, (b) the minimum of ν, and (c) the phase separation $\Delta\sigma$ for the low-amplitude case, $\psi_0 = 0.02$. The parameters are $u = 0.4$, $K_0 = 0.19$, and $K_{z0}/K_{x0} = 0.1$. The spatial resolution is 16×16 Fourier modes.

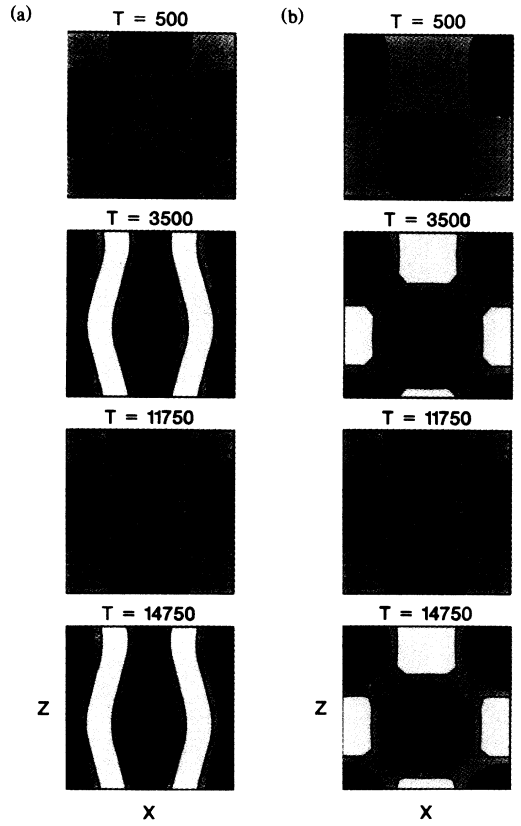

FIG. 2. The evolution of the spatial structures of (a) $|\psi|^2$ and (b) ν for the same parameters as in Fig. 1. The size of the spatial domain is $L_x = 2\pi/K_{x0} = 33.07$ and $L_z = 2\pi/K_{z0} = 330.7$. The darkest shading denotes the highest (positive) values. In (a) the contours are drawn at the values $(2, 4, \text{and } 6) \times 10^{-4}$ and in (b) the contours correspond to $(-2, 0, \text{and } +2) \times 10^{-3}$.

equations, at least for the time duration (the first recurrence period) they have studied. In the growing phases of the modulation, the evolution is in accordance with the linear predictions [Eqs. (3) and (4)]. The modulation has a spatial structure resembling cells stretched and propagating along the z axis, with the maximum of $|\psi|^2$ roughly $L_z/4$ ahead of the minimum of v as seen in Fig. 1(c), which shows the phase separation, $\Delta\sigma$, between the fundamental components [(1,1) mode] of $|\psi|^2$ ($\approx \psi_0^2 + 2|\phi|\psi_0$) and v. The termination of the growth is associated with a further stretching of the spatial structure of $|\psi|^2$ along the z axis, which gives rise to a dip in $|\psi|^2_{\max}$. The v cells conserve their symmetry. Then $\Delta\sigma$ changes and during the decreasing periods of the modulation the maximum of $|\psi|^2$ is $3L_z/4$ ahead of the minimum of v. When the modulation has almost died out the phase gently slides back to fulfill the condition for growth, cf. Eqs. (4), and the modulation starts growing again. The recurrent behavior observed in Figs. 1 and 2 may be described by a simplified model based on a generalized Hamiltonian formulation of Eqs. (1) and (2), which is truncated to involve only a few modes.[10]

For increasing initial amplitude the recurrent feature gets less pronounced and the spreading of the energy to higher mode numbers proceeds faster. This behavior is exemplified in Figs. 3 and 4, where the initial amplitude has been raised to $\psi_0 = 0.04$. Initially we observe an evolution similar to the one observed in Figs. 1 and 2 with one period of almost perfect recurrence. The time scale of the evolution is approximately half the one observed in Fig. 1, in agreement with the prediction that the growth rate is roughly proportional to the amplitude [Eq. (3)]. During that initial phase the main part of the energy is still residing in the fundamental mode as seen in Fig. 4. Note that the peak at $K_z = 0$, $K_x = 2K_{x0}$ in the $|\psi|^2$ spectrum [Fig. 4(a)] corresponds to a stretching of the $|\psi|^2$ cells at the termination of the growth as also seen in Fig. 2(a). After the decreasing phase, with $\Delta\sigma \approx +L_z/4$ as in Fig. 1(c), the modulation does not com-

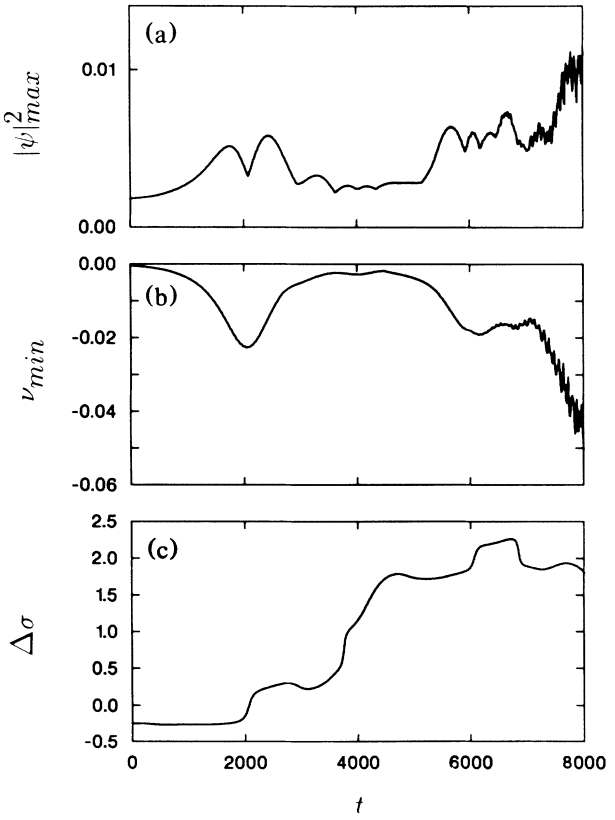

FIG. 3. The evolution of the maximum of (a) $|\psi|^2$, (b) the minimum of v, and (c) $\Delta\sigma$ for the high-amplitude case, $\psi_0 = 0.04$. The spatial resolution is 32×32 Fourier modes. The other parameters are as in Fig. 1.

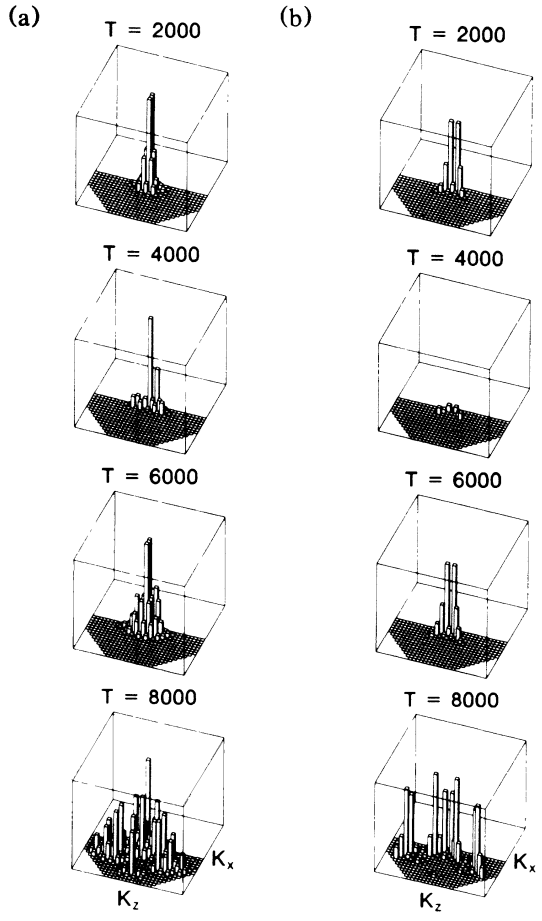

FIG. 4. The amplitude spectra of (a) $|\psi|^2(\mathbf{K})$ and of (b) $v(\mathbf{K})$ at different times for the same parameters as in Fig. 3. Only half of the K space is shown; the other half is obtainable from the reality condition [e.g., $v(\mathbf{K}) = v^*(-\mathbf{K})$]. The fundamental mode is $(K_{x0}, K_{z0}) = (0.19, 0.019)$. The vertical size of the box corresponds to 5×10^{-4} in (a), where the maximum value attained by the (0,0) mode (the carrier wave) is 1.6×10^{-3}, and to 4.43×10^{-3} in (b), which is equal to the maximum value.

pletely reach its initial value and there resides a non-negligible energy in modes other than the fundamental. For larger times the modulation regrows in a rather irregular fashion (compare Figs. 1 and 3), due to the involvement of the higher modes. However, the growth of the fundamental mode dominates the evolution [Fig. 4(b)]. It roughly follows the linear prediction with respect to the phase separation $\Delta\sigma$ [Fig. 3(c)] and the growth rate [Fig. 3(b)]. For larger times, progressively higher modes get involved in the process as seen in Fig. 4. Note that while the dominant modes in the $\nu(\mathbf{K})$ spectrum for small mode numbers satisfy $K_z/K_x = K_{z0}/K_{x0} = 0.1$, for higher mode numbers the relation becomes $K_z/K_x \approx 0.15$ indicating that the cell structures in configuration space become less stretched along the z axis. The observed development indicates that the energy will ultimately cascade to arbitrary high wave numbers giving rise to an apparently chaotic or random wave field. Taking account of additional effects,[11] which, e.g., allow for leakage of the whistler waves from the density ducts with scale length comparable to the whistler wavelength, or account for the dispersion of the low-frequency MHD waves may hinder the spreading of the energy to the higher mode numbers.

By inspection of the linear dispersion relations for the MI we found that the dominant higher modes in the low-amplitude case and in the high-amplitude case for $T \leq 6000$, i.e., the "direct" harmonics (nK_{x0}, mK_{z0}) with $n=m$ and also the $(K_z=0, K_x=nK_{x0})$, are all stable. Thus, the spreading of the energy is solely caused by nonlinear effects during the initial time. Some of the higher modes with $m > n$, excited at later times in the high-amplitude case [Fig. 4(b)], are linearly unstable, however, which explains their rapid appearance; recall that the maximum growth rate increases with K [Eq. (3)]. For other parameters, e.g., smaller K values, these nonlinearly excited "direct" harmonics may be linearly unstable. Consequently, the spreading of the energy to higher wave numbers becomes more effective and the recurrent feature becomes less pronounced. We have, for instance, observed that even for the low-amplitude case $\psi_0 = 0.02$ only one recurrence period exists for cases where $(2K_{z0}, 2K_{x0})$ is linearly unstable.

In conclusion, we have found that the two-dimensional MI of whistler waves generally evolves in a quasirecurrent manner with the main part of the energy residing in the fundamental mode and a slow spreading of energy to higher mode numbers. The detailed evolution depends on the initial conditions and the spreading of energy proceeds faster for higher amplitudes and/or when the "direct" harmonics of the initial modulation are unstable. Recurrence is in general expected to occur in bounded systems having a finite number of "effective" degrees of freedom.[12] By using the conserved quantities of Eqs. (1) and (2), I_1 and the Hamiltonian,[10] we have attempted to estimate an upper bound on the number of "effective" modes[12] for our system, but without any definite result.

The recurrent behavior indicates the possibility of the existence of narrow-band modulated whistler-wave trains resulting from the MI, and indeed a spectrum with few discrete sidebands similar to what has been observed in active experiments in the magnetosphere[4] can be reproduced. Whistlers with amplitude of the same order of magnitude as used in Figs. 1 and 2 have been observed.[3] For that case the recurrence period ($T \approx 6000$) corresponds to ≈ 0.1 s for a typical magnetospheric whistler wave of frequency 10 kHz. This time is shorter than the wave transit time (≤ 1 s) through the equatorial region of the magnetosphere; thus, the effect should be observable.

This work was initiated while one of the authors (V.I.K.) stayed at Risø National Laboratory. He acknowledges the support of this institution and is grateful for the warm hospitality of his collaborators. We thank G. Knorr for useful discussions.

[a]Permanent address: IZMIRAN, Academic City, Moscow Region 142092, U.S.S.R.

[1]V. I. Karpman and H. Washimi, J. Plasma Phys. **18**, 173 (1977); L. Stenflo, M. Yu, and P. K. Shukla, J. Plasma Phys. **36**, 447 (1986).

[2]V. I. Karpman and A. G. Shagalov, J. Plasma Phys. **38**, 155 (1987); **39**, 1 (1988).

[3]P. K. Shukla, Nature (London) **274**, 874 (1978).

[4]T. F. Bell, J. Geophys. Res. **90**, 2792 (1985).

[5]V. I. Karpman and L. Stenflo, Phys. Lett. A **127**, 99 (1988).

[6]B. M. Lake, H. C. Yuen, H. Rungaldier, and W. E. Ferguson, J. Fluid Mech. **83**, 49 (1977); H. C. Yuen and W. E. Ferguson, Phys. Fluids **21**, 1275 (1978).

[7]D. U. Martin and H. C. Yuen, Phys. Fluids **23**, 881 (1980).

[8]V. I. Karpman, Phys. Lett. A **136**, 216 (1989); **136**, 221 (1989).

[9]E. A. Coutsias, F. R. Hansen, T. Huld, G. Knorr, and J. P. Lynov, Phys. Scr. **40**, 270 (1989).

[10]V. I. Karpman, Phys. Lett. A **137**, 379 (1989); V. I. Karpman *et al.*, Phys. Lett. A **139**, 423 (1989).

[11]V. I. Karpman, R. N. Kaufman, and A. G. Shagalov, J. Plasma Phys. **31**, 209 (1984); V. I. Karpman and A. G. Shagalov, J. Plasma Phys. **41**, 289 (1989).

[12]A. Thyagaraja, in *Nonlinear Waves*, edited by L. Debnath (Cambridge Univ. Press, New York, 1983), pp. 308–325.

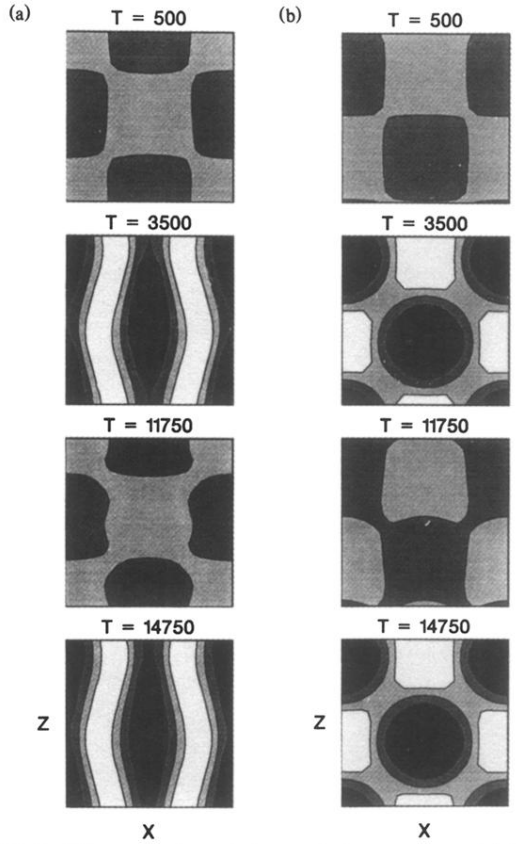

FIG. 2. The evolution of the spatial structures of (a) $|\psi|^2$ and (b) v for the same parameters as in Fig. 1. The size of the spatial domain is $L_x = 2\pi/K_{x0} = 33.07$ and $L_z = 2\pi/K_{z0} = 330.7$. The darkest shading denotes the highest (positive) values. In (a) the contours are drawn at the values $(2, 4, \text{and } 6) \times 10^{-4}$ and in (b) the contours correspond to $(-2, 0, \text{and } +2) \times 10^{-3}$.